

Work function of small metal particles: Self-consistent spherical jellium-background model

W. Ekardt

Fritz-Haber-Institut der Max-Planck-Gesellschaft, Faradayweg 4-6, D-1000 Berlin 33, Germany

(Received 11 August 1983)

The work function of small metal particles is calculated with the use of the local-density approximation applied to the spherical jellium-background model. Large quantum-size effects are obtained in strict analogy to those obtained for thin metal films. Effective potentials and self-consistent charge densities are discussed in comparison to the semi-infinite half-space. The convergence of the various physical properties to their value of a semi-infinite half-space is investigated.

I. INTRODUCTION

In a recent paper Martins *et al.*¹ studied the ionization potential (IP) and the electron affinity (EA) of small metal particles within the local-density approximation (LDA) applied to the spherical jellium-background model (SJBm). Owing to the existence of a pronounced curvature at the surface of small particles a self-consistent determination of the charge density both of the neutral cluster and of the singly ionized one seems to be very important. For a non-self-consistent calculation, one can obtain a wrong value for the Coulomb energy of the system, which is usually thought to give an important contribution to the work function of these small metallic clusters.² Therefore, it is highly desirable to repeat the calculations of Martins *et al.*¹ in a strictly self-consistent fashion instead of using a trial potential whose parameters are determined variationally.^{2,3}

The resulting work function consists of three different contributions, namely the kinetic part, the exchange-correlation part, and the electrostatic part. Whereas the first two contributions approach the chemical potential of the infinite bulk solid, the latter contribution approaches the surface-barrier part of the work function of the infinite half-space. A study of these three different parts as a function of the size of the cluster can then reveal whether or not the electrostatic part of the work function is the important one in producing the size effect.²

The results to be expected from the self-consistent SJBm must, however, be considered with care. In the case of a cluster consisting of a few numbers of atoms the geometrical structure of the ions is an important ingredient for any cluster calculation which is completely neglected in the SJBm. For such low numbers of atoms a realistic charge density can only be obtained by more sophisticated models such as the self-consistent-field $X\alpha$ scattered wave (SCF- $X\alpha$ -SW) method⁴ or some other method.⁵ However, for a large number of atoms within the cluster these methods cannot be applied successfully and one has to resort to some much simpler model, e.g., the SJBm. In this case, the model should be reasonable since a large polyhedron can always be approximated by a sphere. The remaining lattice effects can be reintroduced

by pseudopotential perturbation theory in a fashion similar to that proposed originally by Perdew *et al.*⁶

Our main intention with the present model is its further use in the calculation of the optical properties of small metallic aggregates. In this case any molecular approach is far too complicated, and therefore a model such as the one presently under study seems to be the only tractable microscopic approach in the case of a larger number of particles.

II. THEORY

The starting point of our discussion is the energy functional $E[\rho]$ defined by⁷

$$E[\rho] = E_{\text{kin}}[\rho] + E_{\text{xc}}[\rho] + E_{\text{es}}[\rho], \quad (1)$$

where E_{kin} , E_{xc} , and E_{es} are, respectively, the kinetic, the exchange-correlation, and the electrostatic part of the total energy of the system under consideration.

In the case of the SJBm the electrostatic part E_{es} is given by

$$E_{\text{es}}[\rho] = \int \int d\vec{r} d\vec{r}' \frac{[\rho(\vec{r}) - n^+(r)][\rho(\vec{r}') - n^+(\vec{r}')] }{|\vec{r} - \vec{r}'|}, \quad (2)$$

with

$$n^+(\vec{r}) = n_0(r_s^0)\Theta(R - r) \quad (3)$$

the homogeneously smeared-out density of positive ions. Here, $\Theta(x)$ is the unit step function, R is the particle radius, and $n_0(r_s^0)$ is the constant bulk density pertaining to a metal with $r_s^0 = (3/4\pi n_0)^{1/3}$. The exchange-correlation part of the total energy is usually taken into account in LDA. Following Gunnarsson and Lundqvist,⁸ the following interpolation form is used for the exchange-correlation part of the total energy

$$E_{\text{xc}} = \int d\vec{r} \rho(\vec{r}) \epsilon_{\text{xc}}(\rho(\vec{r})), \quad (4)$$

with

$$\epsilon_{xc}(\rho(\vec{r})) = -0.916/r_s(\vec{r}) - 0.0666G\left(\frac{r_s(\vec{r})}{11.4}\right). \quad (5)$$

Here, $G(x)$ is defined by

$$G(x) = \left[\left(1+x^3\right) \ln \left[1 + \frac{1}{x} \right] - x^2 + \frac{x}{2} - \frac{1}{3} \right], \quad (6)$$

and $r_s(\vec{r}) = [3/4\pi\rho(\vec{r})]^{1/3}$ is the local r_s value. Finally, the kinetic part of the total energy,

$$E_{\text{kin}} = \sum_{i=1}^N \langle i | -\Delta | i \rangle = \sum_{i=1}^N \epsilon_i - \int d\vec{r} \rho(\vec{r}) V(\vec{r}; \rho(\vec{r})), \quad (7)$$

can be obtained exactly by solving the following set of equations self-consistently:⁹

$$[-\Delta + V(\vec{r}; \rho(\vec{r}))]\psi_i(\vec{r}) = \epsilon_i \psi_i(\vec{r}), \quad (8)$$

$$\rho(\vec{r}) = \sum_{i=1}^N |\psi_i(\vec{r})|^2, \quad (9)$$

$$V(\vec{r}) = V_H(\vec{r}; \rho(\vec{r})) + V_{xc}(\rho(\vec{r})), \quad (10)$$

$$V_H(\vec{r}) = 2 \int d\vec{r}' \frac{\rho(\vec{r}') - n^+(\vec{r}')}{|\vec{r} - \vec{r}'|}, \quad (11)$$

$$V_{xc}(\vec{r}) = \frac{d}{d\rho} [\rho \epsilon_{xc}(\rho)] \\ = -1.222/r_s(\vec{r}) - 0.0666 \ln \left[1 + \frac{11.4}{r_s(\vec{r})} \right]. \quad (12)$$

Equations (8)–(12) were solved for $r_s^0 = 4$ (the bulk value of Na) for particle numbers up to 168. The calculations were performed for the neutral cluster as well as for a pos-

itive, singly ionized one. In this fashion, the size-dependent IP was obtained.

The experimentally confirmed lattice shrinkage¹⁰ could be incorporated in the model by changing r_s^0 to $r_s^0(R)$. In addition, a shell-dependent shrinkage may be introduced by a r -dependent r_s^0 value.

This and related problems are deferred to another paper as is the refinement of the model by using the local-spin-density approximation⁸ instead of the LDA. We shall come back to this point in the discussion of our results.

III. RESULTS AND DISCUSSIONS

One of the most important physical properties of small metal clusters (compared to an infinite, flat surface) is the IP and its convergence to the work function of the corresponding metallic half-space. Figure 1 shows what happens. First of all, a strong oscillatory behavior is observed which can be attributed to the spherical shell structure of the problem.

Whenever a shell is completely filled the work function is at a maximum, reflecting a strong exchange-correlation-enhanced binding of the last electron filling this shell. The convergence to the work function at $R = \infty$ is rather slow and the reason for this is simply the high orbital degeneracy at larger values of the angular quantum number l . This effect will be weakened by going from the LDA to the local-spin-density approximation. In addition, the experimentally well-documented odd-even effect¹¹ of the IP will be reproduced after spin effects have been included.

In sharp contrast to the strong oscillations of the *total* IP the electrostatic part of it, $\Delta_{\text{IP}}^{\text{es}}$, defined as follows,

$$E_{\text{IP}} = E_{\text{tot}}^+(N-1) - E_{\text{tot}}^{\text{neutral}}(N) = E_{\text{es}}^+(N-1) - E_{\text{es}}^{\text{neutral}}(N) - [E_{\text{kin}}^{\text{neutral}}(N) + E_{\text{xc}}^{\text{neutral}}(N) - E_{\text{kin}}^+(N-1) - E_{\text{xc}}^+(N-1)] \\ \equiv \Delta_{\text{IP}}^{\text{es}} - \bar{\mu}(N), \quad (13)$$

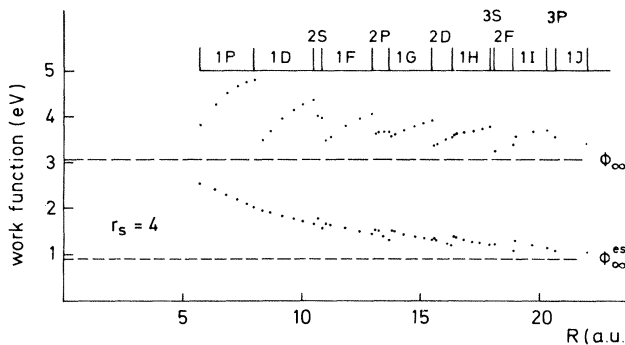


FIG. 1. Work function of small metal particles as calculated in the self-consistent SJBm. R is the particle radius, $R = r_s N^{1/3}$ with N the number of particles. ϕ_∞ is the work function of the infinite, flat surface. ϕ_∞^{es} is the electrostatic part of ϕ_∞ , sometimes called χ , the electrostatic surface barrier. $1p$, $1d$, $2s$, etc., are the quantum numbers of the spherical potential hole. $1p$ is the lowest state with $l=1$, and $2s$ is the second state with $l=0$, etc. The results for the $1s$ shell are not shown. The cluster with a completely filled $1j$ shell contains 168 electrons. $r_s=4$ is the mean bulk density of Na. Whereas the total work function shows pronounced shell effects, the electrostatic part of it behaves rather smoothly.

shows rather smooth behavior. However, the size effect of $\Delta_{\text{IP}}^{\text{es}}$ is not as strong as would be expected on the basis of a classical electrostatic model. Herrmann *et al.*¹¹ predict for this effect an enhancement of the work function by an amount of $e^2/2R$, which gives a value of 0.68 eV at $R=20$ a.u. Owing to the spatial distribution of the missing charge over the whole sphere, this effect is strongly re-

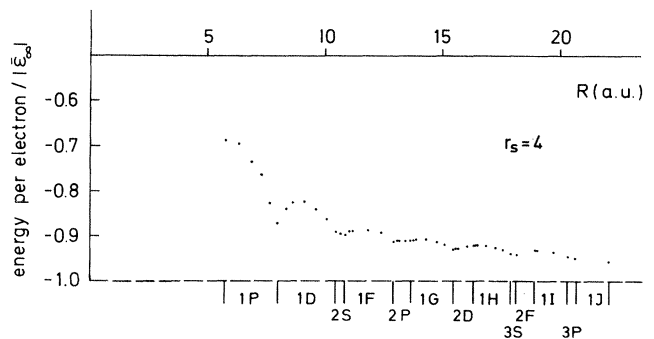


FIG. 2. Size dependence of the mean energy per electron of a neutral cluster in units of the magnitude of the bulk value $|\epsilon_\infty|$. For further discussion see text.

duced, resulting in an extraelectrostatic contribution to the ionization potential of ~ 0.2 eV at $R \sim 20$ a.u. On the other hand, the overall convergence of $\Delta_{\text{IP}}^{\text{es}}$ to the electrostatic surface barrier χ of a metal with $r_s^0 = 4$ can easily be seen.¹²

Another physical property of interest is the mean energy per particle and its convergence to its bulk value. Figure 2 shows that shell effects of E_{tot}/N are not as strong as in the case of the IP. The bulk value of E_{tot}/N is roughly attained for $N = 140$.

The slow convergence of all the physical properties as

calculated in the SJBM is undoubtedly caused in part by the very high degeneracy of the angular-moment states (i.e., by the high symmetry of the model). However, first-principles calculations on Ni_{13} – Ni_{87} by Melius *et al.*¹³ show a similar trend. In this case the IP of a Ni_{43} cluster is 5.1 eV (compared to 5.2 eV of the work function of the infinite half-space). But the IP shows still strong oscillation upon the addition of further shells of a fcc cluster: The IP for Ni_{55} (four shells) is equal to 5.52 eV, and that for Ni_{79} (five shells) is 5.92 eV. An abrupt change is obtained after adding the sixth shell: The IP for Ni_{87} equals

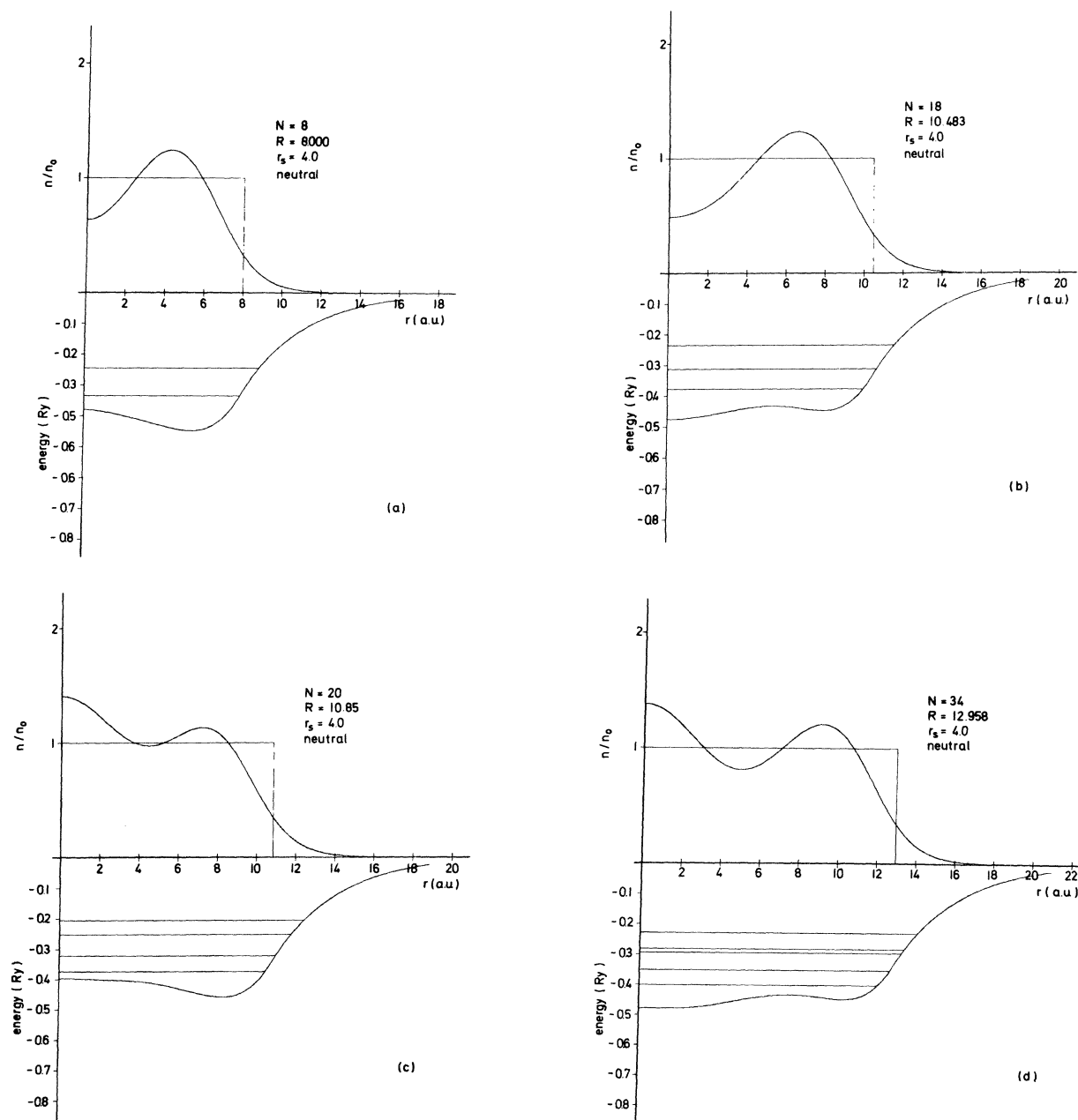


FIG. 3. Evolution of the charge density as a function of size. Given is the total $n(r)/n_0$ after the various shells have completely been filled. For the highest particle number studied, $N = 198$, the charge density across the surface looks very similar to that at $R = \infty$. However, $n(r)$ inside the cluster still looks rather different from n_0 . For further discussion see text.

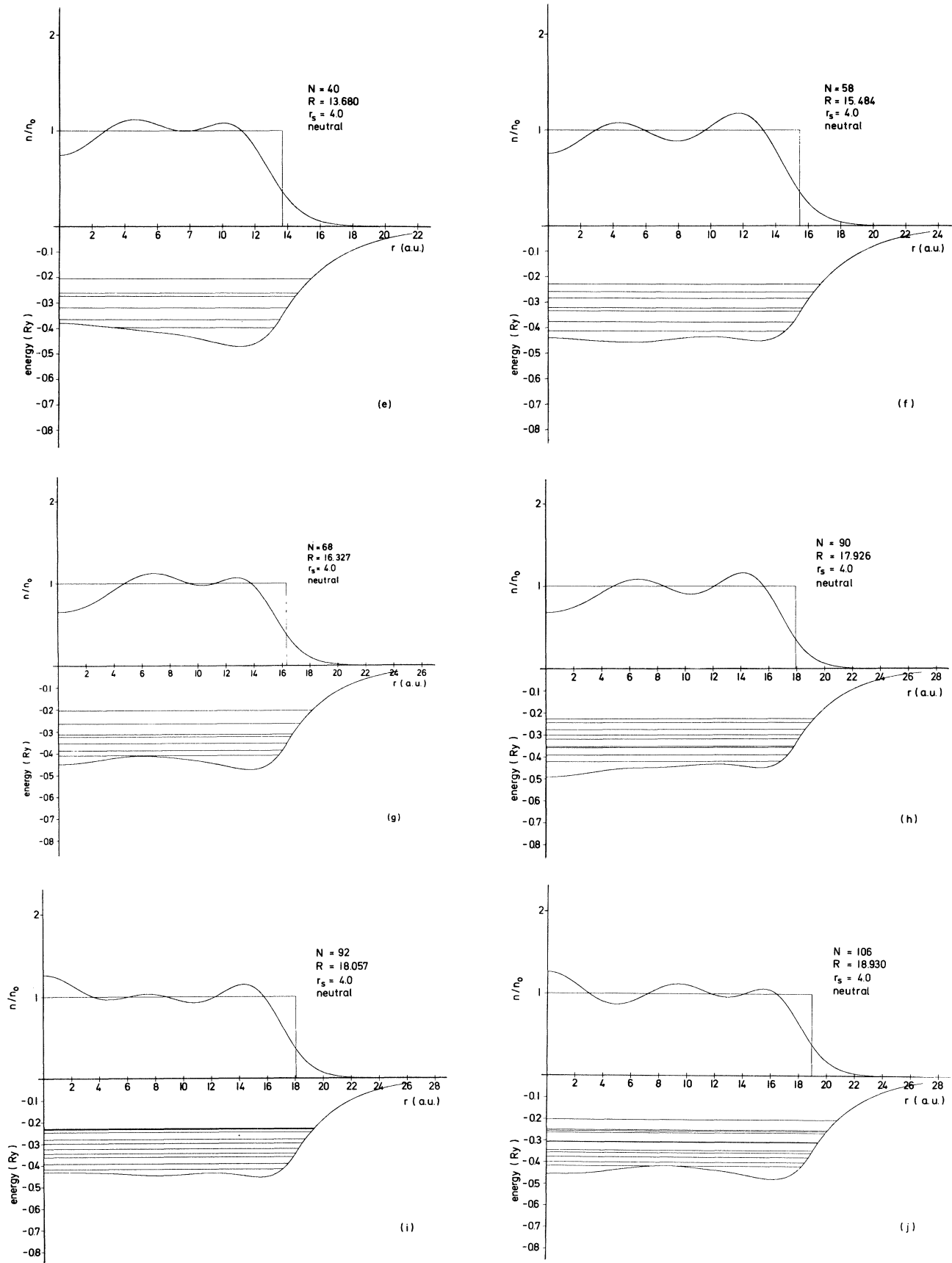


FIG. 3. (Continued.)

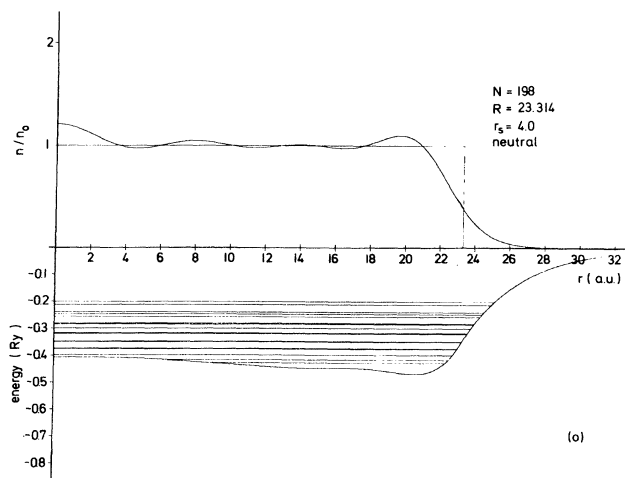
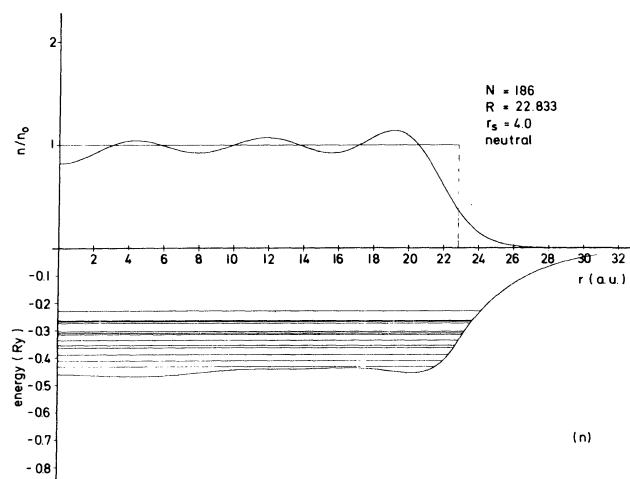
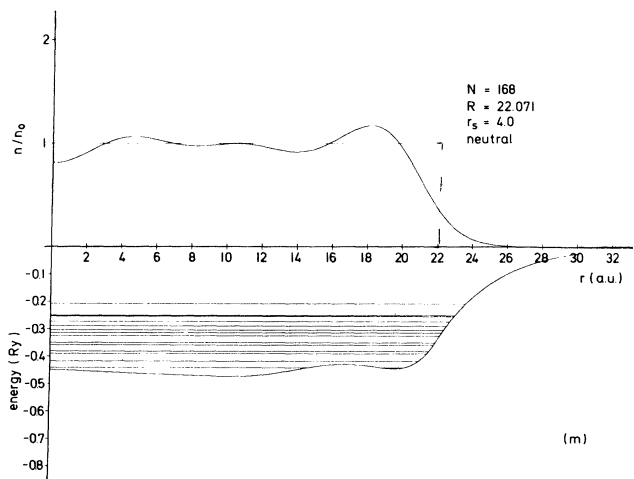
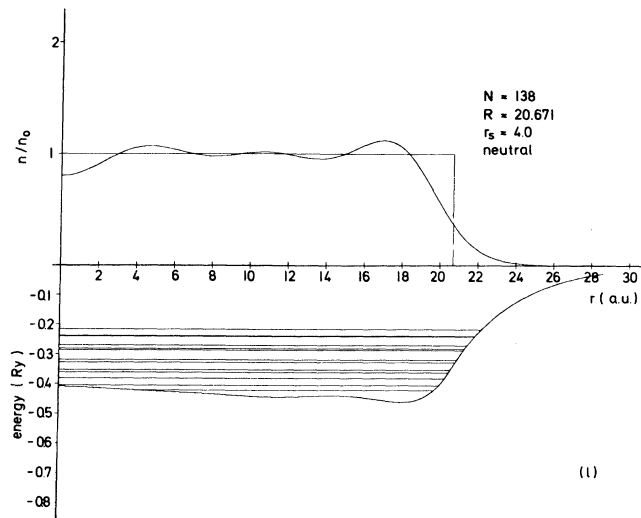
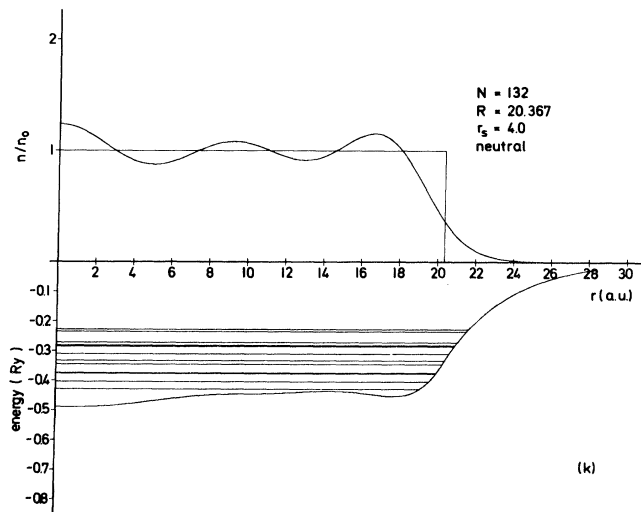


FIG. 3. (Continued.)

4.86 eV. We therefore conclude that the shell structure of the physical properties might be a real effect of small metal clusters whose magnitude, however, depends on the model used.

Another interesting feature is the behavior of both the self-consistent charge density and the self-consistent effective one-particle potential when the number of atoms within the cluster is raised. Figure 3 shows the charge density, the level structure, and the effective potential of the various completely filled shells of the neutral cluster. There are two striking features. First, the charge density around the center of the sphere is determined by the number of s electrons. Owing to the boundary conditions to be fulfilled at $r=0$, all the other electrons are repelled from the center of the sphere. After a certain s shell has been filled ($1s, 2s, 3s$, and $4s$) the charge density around $r=0$ monotonically decreases due to the increasingly extended nature of these (normalized) states. On the other hand, the behavior of the charge density across the surface ($r=R$) is nearly the same for all R values studied. This is in agreement with a variational study of the size-dependent total energy of the cluster in which an exponential-type density was used.¹⁴ The decay parameter of the charge density outside the sphere, $\sim e^{-\beta r}$, approaches its bulk value¹⁵ ($R \rightarrow \infty$) extremely slowly. More important seems to be the charge-reorganization effect when the various shells are filled. For the uppermost particle number studied, $N=198$, the outer part of the charge density, $r \gtrsim 12$ a.u., looks very much like the Friedel oscillations observed for an infinite, flat surface (but with a different decay parameter), whereas the interior part of the charge density does not yet approach a constant value. This behavior of the charge density sheds doubt on the usefulness of some concepts concerning the calculation of the optical properties of small metallic particles,^{16,17} which start from the behavior at $R = \infty$ and take into account the curvature of the sphere merely to first order of $1/R$. Both the charge density and the effective potential seem to indicate that it is important to calculate the dielectric susceptibility of small metallic particles on the basis of the level structure shown in the figure. Surprisingly enough, the electrostatic part of the IP approaches its bulk value already at $N \approx 170$, whereas the charge density still looks rather different to the infinite surface charge density. This behavior indicates some cancellation of size effects in the difference of the two total energies from which the electrostatic part of the IP is calculated, namely $E_{\text{tot}}^+(N-1)$ and $E_{\text{tot}}^{\text{neutral}}(N)$. This conclusion is supported by comparing the charge densities of the neutral cluster and of the single ionized one. This comparison is shown in Fig. 4 for $N=60$. The missing charge of the ionized cluster acts like a rigid shift of the potential *inside* the cluster: Except for a constant, the two level schemes are nearly identical as is the overall appearance of the two charge densities. The reason for this peculiar behavior is simply the extended nature of the orbital of the missing electron. Of course, the potential difference *outside* the cluster is not a constant because the potential of the singly ionized cluster approaches the Coulomb potential $-2/r$.

Similar behavior is observed for the ionization of the

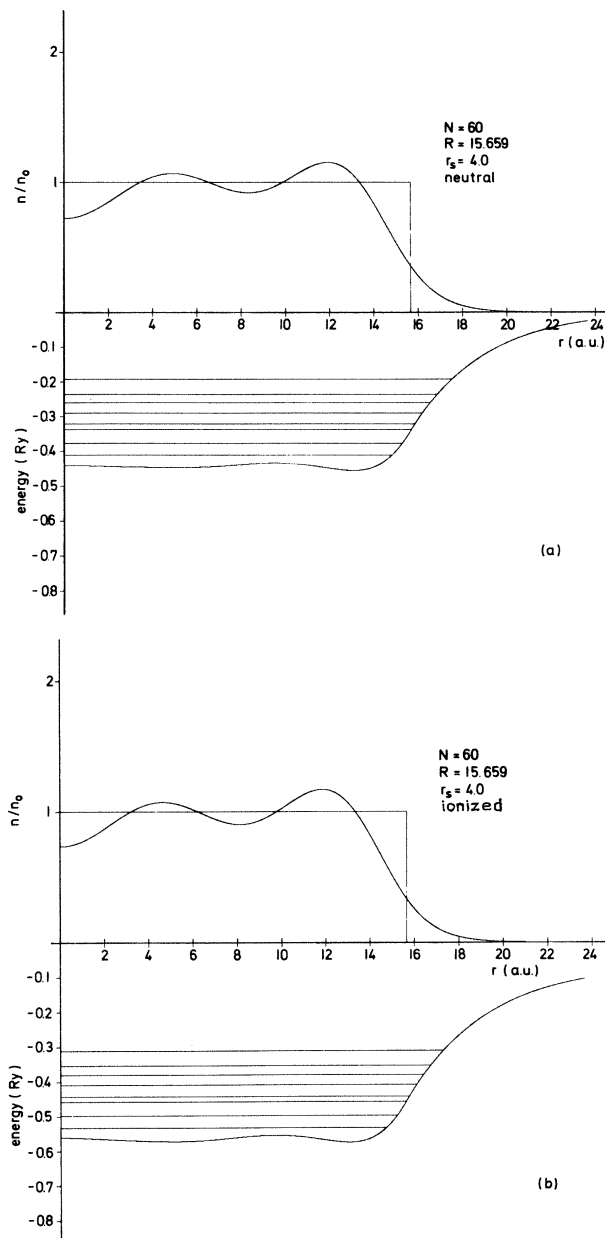


FIG. 4. Comparison of $n(r)$ for the neutral cluster and the singly ionized one. The missing electron causes, inside the cluster, a nearly rigid potential shift. Therefore, the two level structures are very similar.

deeper lying states within the valence band. There is almost no additional relaxation (compared to the uppermost filled level), again due to the extended nature of all the orbitals within the cluster. It is only in the case of a very few number of atoms that this complication comes into play.

Finally, we want to compare our results with the work of Martins *et al.*,¹ which gave impact to the present study. Unfortunately, probably the most sensitive physical property of the cluster, namely the behavior of the charge density, was not published in Ref. 1. It is known that the Friedel oscillations of the electronic charge across the surface are *sensitively* dependent on the potential used

in calculating them. A comparison of the self-consistently calculated charge density with the variationally determined one would, therefore, most clearly reveal the importance of a self-consistent model. Owing to the lack of information about this point we are forced to compare the two models by looking at an integral property, e.g., the IP, which is invariably less sensitive to the model used to calculate it. Upon comparing Fig. 1 of Ref. 1 with Fig. 1 of the present paper we see immediately that both quantitative and qualitative differences in the size dependence of the IP exist. For instance, the IP within the $2p$ shell is strongly size dependent in a non-self-consistent model, whereas the IP as calculated in a strictly self-consistent fashion stays nearly constant within that shell. The same applies to the $2d$ shell. The difference would likely be even stronger in the response properties of the metal particle, and such a calculation is presently underway.

IV. CONCLUSION

The SJBM has been investigated with respect to the convergence of the various physical properties to their respective values at an infinite, flat surface. Owing to the high symmetry of the potential, quantum-size effects still exist at a rather large particle number (or radius). However, the electrostatic part of the work function approaches its limiting value in a rather smooth fashion.

Charge densities and self-consistent potentials for particle numbers as large as 170 still deviate from their values across an infinite, flat surface. This behavior, which has already been revealed by a variational calculation, originates from the way in which the levels of a spherical po-

tential are filled. The reintroduction of the lattice structure via pseudopotentials will result in a splitting of the spherical shells. However, a large correction to the simple spherical picture is not to be expected in the case of a high lattice symmetry [for instance Na_{13} with fcc structure (Na and Na_{12})].

This conjecture has already been stated by Geguzin,¹⁸ who compared the results of a non-self-consistent jellium calculation with those following from a SCF- $X\alpha$ -SW calculation. The inclusion of the spin effects by the local-spin-density approximation (at least for a very few number of particles), however, seems to be more important.

The strong deviation of the charge density across the surface from its behavior at $R \rightarrow \infty$ is strongly corroborated by the experimental results concerning the size effects in the behavior of the dipolar collective surface plasmon of small metal particles.¹⁹ In this case, the real part of the frequency already starts to deviate from its classical value $\omega_p/\sqrt{3}$ at a particle radius of about 50 Å (in the case of Ag embedded in an argon matrix).

Finally, we want to stress that the model is not intended to compete with any type of molecular-structure calculations. The results presented above are merely a first step of a DFT-LDA-based solution of the optical-response problem of small metal particles (where DFT denotes density-functional theory).²⁰

ACKNOWLEDGMENTS

Many thanks are due Professor E. Zeitler for his continuing interest and support.

¹J. L. Martins, R. Car, and J. Buttet, *Surf. Sci.* **106**, 265 (1981).
²A. Herrmann, E. Schumacher, and L. Wöste, *J. Chem. Phys.* **68**, 2327 (1978).
³J. H. Rose and H. B. Shore, *Solid State Commun.* **17**, 327 (1975).
⁴J. Harris and G. S. Painter, *Phys. Rev. Lett.* **36**, 151 (1976).
⁵P. S. Bagus, H. F. Schaefer, and C. W. Bauschlicher, *J. Chem. Phys.* **78**, 1390 (1983).
⁶J. P. Perdew and R. Monnier, *Phys. Rev. Lett.* **37**, 1286 (1976).
⁷P. Hohenberg and W. Kohn, *Phys. Rev.* **136**, B864 (1964).
⁸O. Gunnarsson and B. I. Lundqvist, *Phys. Rev. B* **13**, 4274 (1976).
⁹W. Kohn and L. J. Sham, *Phys. Rev.* **140**, A1133 (1965).
¹⁰G. Apai, J. F. Hamilton, J. Stöhr, and A. Thompson, *Phys. Rev. Lett.* **43**, 165 (1979).
¹¹A. Herrmann, E. Schumacher, and L. Wöste, *J. Chem. Phys.*

68, 2327 (1978).

¹²N. D. Lang and W. Kohn, *Phys. Rev. B* **3**, 1215 (1971).

¹³C. F. Melius, T. H. Upton, and W. A. Goddard III, *Solid State Commun.* **28**, 501 (1978).

¹⁴W. Ekardt (unpublished results).

¹⁵J. R. Smith, *Phys. Rev.* **181**, 522 (1969).

¹⁶A. Ljungbert and P. Apell, *Solid State Commun.* **46**, 47 (1983).

¹⁷P. Apell and D. R. Penn, *Phys. Rev. Lett.* **50**, 1316 (1983).

¹⁸I. I. Geguzin, *Fiz. Tverd. Tela (Leningrad)* **24**, 494 (1982) [*Sov. Phys.—Solid State* **24**, 248 (1982)].

¹⁹W. Ekardt, D. B. Tran Thoai, F. Frank, and W. Schulze, *Solid State Commun.* **46**, 571 (1982) [*Sov. Phys.—Solid State* **24**, 248 (1982)].

²⁰First results were presented at the Discussion Meeting "Experiments on Clusters" [*Ber. Bunsenges. Phys. Chem.* (in press)].